Lithium Dynamics in Molybdenum Disulfide Intercalation Compounds Studied by Nuclear Magnetic Resonance

José Pedro Donoso, Claudio José Magon, José Schneider, Antonio Carlos Bloise,
IFSC, Universidade de São Paulo,13560-970 São Carlos, S.P. Brazil

Eglantina Benavente,
Universidad Tecnológica Metropolitana, Av. J.P. Alessandri 1242, Santiago, Chile

Víctor Sanchez, Maria Angélica Santa Ana, and Guillermo González
Facultad de Ciencias, Universidad de Chile, PO Box 653, Santiago, Chile

Cluster architecture and lithium motion dynamics are investigated in nanocomposites formed by the intercalation of lithium and a dialkylamine (diethylamine, dibutylamine and dipentylamine) in molybdenum disulfide by means of ^{7}Li Nuclear Magnetic Resonance (NMR) technique. The present contribution illustrates the potential of the NMR techniques in the study of both the short range atomic structure and the local dynamics of ions in these intercalation compounds. Structural information is gained through measurements of the various interactions (such as dipolar and quadrupolar) that affect the lineshapes of the NMR spectra, while ion dynamics information is gained through the study of the effects that ionic motion has on the nuclear relaxation times, which are modulated by these interactions. The formation of lithium clusters in these nanocomposites is suggested by the Li-Li dipolar interaction strength calculated from the ^{7}Li NMR data. The lithium spin-lattice relaxation is mainly due to the interaction between the quadrupolar moment of the ^{7}Li nuclei and the fluctuating electric field gradient at the site of the nucleus, produced by the surrounding charge distribution. The relaxation mechanism is consistent with a fast exchange motion of lithium ions between the coordination sites within the aggregates.

Keywords: NMR; Lithium dynamics

I. INTRODUCTION

Solid-state nuclear magnetic resonance (NMR) has proven to be a powerful tool for the study of complex motions on a microscopic scale, since both conformational and dynamical properties may be obtained. As an element-selective method, sensitive to local interactions, as homo- and hetero- dipolar interactions and nuclear electric quadrupolar couplings, NMR line shapes and relaxation time studies can provide valuable information on the atomic and molecular motions that modulate these interactions [1-6].

Interpretation of NMR relaxation measurements is not always straightforward, however. One of the requisites to extract detailed dynamic information from the NMR studies is to determinate the interactions responsible for the relaxation process. The dominant nuclei interactions in ionic conductors and molecular solids are: (1) magnetic interactions which couple to the nuclear magnetic dipole moments, and (2) quadrupolar interactions which accounts for the interaction between the non-cubic electric field gradient (EFG) at the nuclear site and the quadrupole moment of the nucleus with spin $I \geq 1$.

In the present contribution we probe ^{7}Li ($I = 3/2$) to illustrate the potential of the NMR techniques to study the molecular architecture and lithium dynamics in nanocomposite formed by the co-intercalation of lithium and dialkylamines in molybdenum disulphide. In the last decade, there has been growing the interest in intercalation compounds based

on transition metal dichalcogenides because of their potential applications as electrodes in solid-state batteries [7-9]. Additionally, the study of the dynamics of the species intercalated in layered materials constitutes one interesting problem in the field of solid-state physics. A number of recent studies have been addressed to the arrangements and the dynamics of species confined in low-dimensional spaces [10-17].

In a previous study we reported a carbon (^{13}C), proton (^{1}H) and lithium (^{7}Li) NMR investigation of the nanocomposite formed by the intercalation of lithium and diethylamine into molybdenum disulphide, $Li_{0.1}MoS_2[C_4H_{10}NH]$ [18]. Here, we extend this study to include the nanocomposites prepared with larger amines, such as $C_8H_{18}NH$ (dibutylamine) and $C_{10}H_{22}NH$ (dipentylamine). Our purpose is to provide a more extensive discussion showing how the NMR line shape and relaxation studies can be used to bring up information on both the molecular architecture and the lithium dynamics in these systems.

II. EXPERIMENTAL SECTION

The intercalation of amines into MoS_2 was achieved by the exfoliation of the lithiated molybdenum disulphide. Further details of the sample preparation procedure are given elsewhere [18,19]. The ^{7}Li NMR measurements were performed on a Varian-400 MHz INOVA spectrometer operating at 155.4 MHz using a wide line Varian probe in the temperature range 140-353 K. The static ^{7}Li lineshape was ob-

tained from the Fourier transform of the decaying part of the quadrupolar echo. For the ^{7}Li spin-lattice relaxation time measurements, a saturation-recovery sequence was employed. The heteronuclear dipolar interactions (mainly Li-H) were removed from the ^{7}Li spectra by use of the decoupling technique, performed at 170 K under a magnetic field of 9.4 T, by exciting the ^{1}H nuclear system with the Larmor frequency of 400 MHz. NMR experiments were carried out in the nanocomposites $Li_{0.1}MoS_2[X]_{0.1-0.2}$, where X represents the organic species $C_4H_{10}NH$ (diethylamine), $C_8H_{18}NH$ (dibutylamine) and $C_{10}H_{22}NH$ (dipentylamine), hereafter denoted $Li_{0.1}MoS_2$[d-eth], $Li_{0.1}MoS_2$[d-but] and $Li_{0.1}MoS_2$[d-pn].

III. RESULTS AND DISCUSSION

A. ^{7}Li Static NMR Spectra

Figure 1 shows the low temperature (T = 173 K) static ^{7}Li NMR absorption spectra for the molybdenum disulfide-diethylamine, $Li_{0.1}MoS_2$[d-eth], intercalation compound. Since nuclei with $I > 1/2$ have electric quadrupole moments their NMR spectra and relaxation rates are usually dominated by the interaction of the nuclear quadrupole with the electric field gradients at the nucleus. The NMR powder spectrum of a nucleus with $I = 3/2$ (as ^{7}Li) consists, up to first order in the quadrupolar perturbation, of a dipolar broadened central line associated with the $1/2 \leftrightarrow -1/2$ transition and a symmetric pattern due to the $3/2 \leftrightarrow 1/2$ and $-1/2 \leftrightarrow -3/2$ satellite transitions. The experimental ^{7}Li NMR spectra in Fig. 1 shows a central line superimposed on a broad base line, which is attributed to a distribution of electric field gradients at the lithium sites (i.e., a distribution of the quadrupolar coupling which smear out the quadrupole satellite structure) [4,11].
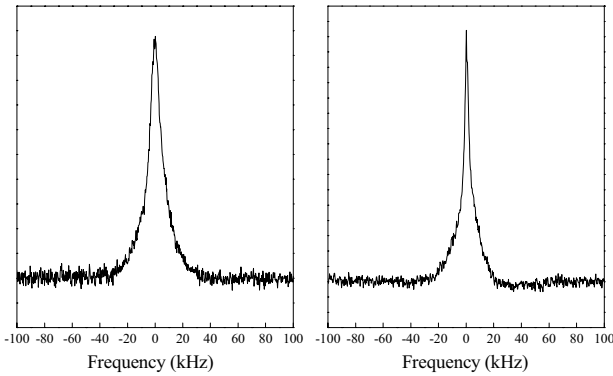

FIG. 1: ^{7}Li NMR spectra of the $Li_{0.1}MoS_2$[d-eth] nanocomposite measured at 173 K. Left: ^{7}Li NMR spectrum; Right: ^{7}Li – $\{^1H\}$ decoupled spectrum. Measurements were taken at the Larmor frequency 155.4 MHz.

The non-decoupled spectrum in Fig. 1 can be adjusted by a superposition of two Gaussian line shapes whose full width at half-height values are in the range 8.5±0.5 kHz, for the central line, and 30±2 kHz, for the baseline, respectively. This last value is a reasonable estimate of the mean quadrupole coupling constant. It should be noted that the second order quadrupolar broadening for an I= 3/2 nuclei with a quadrupole coupling constant of $\sim$30 kHz, is negligible ($\sim$20 Hz) [20]. All the dialkylamine nanocomposites studied in this work exhibit similar baselines. For nuclear spins $I > 1/2$ with small quadrupolar moment (eQ), such as ^{7}Li, the central transition linewidth is primarily determined by dipole-dipole couplings, and it is broadened by homo- and hetero-nuclear dipolar contributions. The heteronuclear interaction affecting the ^{7}Li central line in the dialkylamine nanocomposite is due to amine protons. The homonuclear Li-Li and the heteronuclear Li-H dipolar contributions to the ^{7}Li central line were determined by means of high-power proton decoupling experiments. Fig. 1 shows the ^{7}Li – $\{^1H\}$ decoupled spectra at 173 K of the $Li_{0.1}MoS_2$[d-eth] nanocomposite. The ^{7}Li central line width is reduced to about 50% after proton decoupling without any noticeable effect on the broad base component. The analysis of the ^{7}Li - $\{^1H\}$ decoupled central line, assuming a gaussian shape, leads to a residual line-width value of 4.0±0.5 kHz. Such residual line-width is surprisingly large if compared to the values observed in products of the intercalation of poly(ethylene oxide) in molybdenum disulfide, $Li_{0.1}MoS_2[PEO]_{0.5}$, where the proton decoupling causes a line-width reduction of about 90% [21].

In the low-temperature region where there is no significant ionic motion, commonly referred in NMR terminology as the "rigid lattice", the nuclear second moment of the line is given by Van Vleck's expression, which assumes that the atoms are fixed in well-defined positions. The formalism determines the contribution of the magnetic dipole-dipole interactions to the second moment as a function of the spin of the probed nucleus I, the spin of the other magnetic nuclei S, the number of *like* and *unlike* nuclei whose dipolar interactions are considered, and the inter-nuclear vector r_{ij}. The Van Vleck second moment of the Gaussian lineshape, averaged over all possible orientations of the vector r_{ij} in relation to the magnetic field direction, is inversely proportional to the sixth power of r_{ij} and can be used to estimate the internuclear distances.

The analysis of the ^{7}Li - $\{^1H\}$ decoupled central line of the $Li_{0.1}MoS_2$[d-eth] nanocomposite in Fig. 1, leads to a residual second moment M_2(Li-Li) = 1.1 G^2. Similar results were obtained for the $Li_{0.1}MoS_2$[d-but] and the $Li_{0.1}MoS_2$[d-pn] nanocomposites, whose residual second moments are of the order of $\sim$1.6 G^2. Taking into account the lithium concentration in the nanocomposite samples (0.1 mol Li per mol MoS_2) and assuming a homogeneous distribution of lithium atoms in the sample, the average distance between neighboring ions would be around 7 Å resulting in a second moment calculated by means of the Van Vleck formula of M_2(Li-Li) $\sim 10^{-3}$ G^2. This value is very much smaller than the experimental ones. These results suggest that the lithium atoms are not uniformly distributed in the interlamenar space of the nanocomposites. To explain the strong Li-Li interaction observed in these nanocomposites we proposed that the Li ions are forming aggregates. In the case of the [d-eth] nanocomposite, for example, the formation of a triangular Li_3 species stabilized by amine ligands, with Li-Li distance of about 2.8

Å, was proposed (Fig. 2) [18]. The lithium's tendency to form clusters is well known and the formation of lithium-rich nanoclusters has been reported in several lithium intercalated materials [22-24].
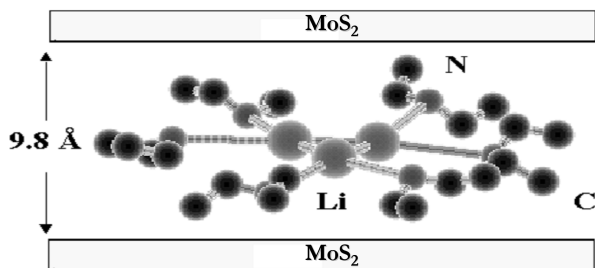

FIG. 2: Structural model proposed for the lithium and the diethylamine cluster co-intercalated in molybdenum disulphide. The self-assembled cluster has a disk shape of 15 Å diameter.

Further support for the proposed structural model for the lithium – diethylamine cluster in Fig. 2 arises from the analysis of the static ^1H NMR absorption spectra. The numerical analysis of the experimental ^1H spectra performed on the basis of the chemical structure of the diethylamine cluster, constituted by the arrangement of NH, CH_2 and CH_3 groups, indicates that the inter-cluster dipole-dipole interactions are responsible for most of the spectral broadening. The second moments parameters determined from the ^1H line-shape analysis were found to be consistent with the measured proton spin-lattice relaxation times [18].

This analysis illustrate, first, how the homo- and heteronuclear dipolar contributions to the ^7Li central line were determined by means of a NMR decoupling experiment; second, how three interactions provided information on the lithum distribution (self-assembling Li_3 clusters) in the interlamenar space of the nanocomposite, and, third, how the measured second moment allow us to determinate the lithium cluster type in the nanocomposite.

Another interesting kind of materials, where the experimental determination of the second moment provides important microscopic structural information, are the fluorogermanate glasses [25]. The low temperature ^{19}F second moments of the glasses $60PbGeO_3-xPbF_2y-CdF_2$, with x + y = 40 and x = 10, 20, 30, 40 (in mol %), indicates that the fluorine ions were not uniformly distributed through the material. The NMR data, along with those of Raman and Exafs, provided the basis for a model of the glass structure at the molecular scale, described by fluorine rich regions permeating the metagermanate chain structures with F-F distances comparable to those found in crystallyne phases [25].

B. ^{7}Li Motional Narrowing

Figure 3 shows the temperature dependence of the ^7Li central transition line-width, without decoupling, in the three $Li_{0.1}MoS_2[X]$ nanocomposites. The linewidth of the ^7Li

line narrows and its shape changes from Gaussian towards Lorentzian with increasing temperature. The line narrowing arises from the dynamic averaging of the ^7Li magnetic dipole-dipole interactions by the lithium ion mobility. As can be seen in Fig. 3, the narrowing onset of the NMR line is shifted from 160 K in the $Li_{0.1}MoS_2[d-eth]$ to 200 K in the $Li_{0.1}MoS_2[d-but]$ and to a still higher temperature in the case of the $Li_{0.1}MoS_2[d-pn]$ nanocomposite. The criterion for motion narrowing is that the rate of fluctuation of the local fluorine dipolar fields, which is generally described in terms of a correlation time τ, become of the much greater than the rigid lattice linewidth expressed in frequency units, i.e. $\tau^{-1} >> (\gamma^2 M_2)^{1/2}$ [26]. One of the interesting features of the data in Fig. 3 is the fact that there is a discernible correlation between the onset of motional narrowing of dialkylamine nanocomposites and the amine size. This point will be further discussed during the analysis of the ^7Li-relaxation.
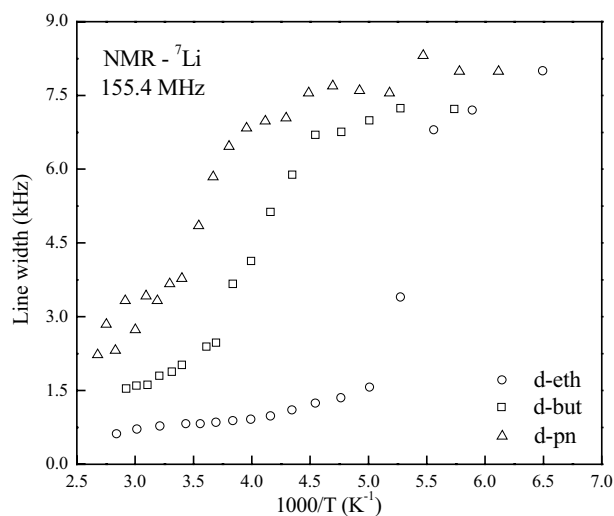

FIG. 3: Temperature dependence of the ^7Li NMR central transition linewidth in the $Li_{0.1}MoS_2[d-eth]$, [d-but] and [d-pn] nanocomposites.

C. ^{7}Li spin-lattice relaxation

NMR spin-lattice relaxation time measurements are often more useful than line-shape analyses to characterize changes of ion and molecular dynamics. The characteristic time window for the ^7Li NMR lineshape analysis ranges between 10^{-3} and 10^{-7} s. Spin lattice relaxation, which perceives the magnetic or electric field gradient fluctuations at the Larmor frequency, extends the sensitive window to much shorter correlation times, down to 10^{-10} s.

Figure 4 shows the temperature dependence of the ^7Li spin-lattice relaxation rates associated to the highly mobile lithium ions of the nanocomposite $Li_{0.1}MoS_2[d-eth]$. As mentioned above, the ^7Li NMR relaxation in ionic solids is mainly governed by two mechanisms: (i) quadrupolar relaxation $(T_1^{-1})_Q$ due to the interaction between the quadrupole moment of the
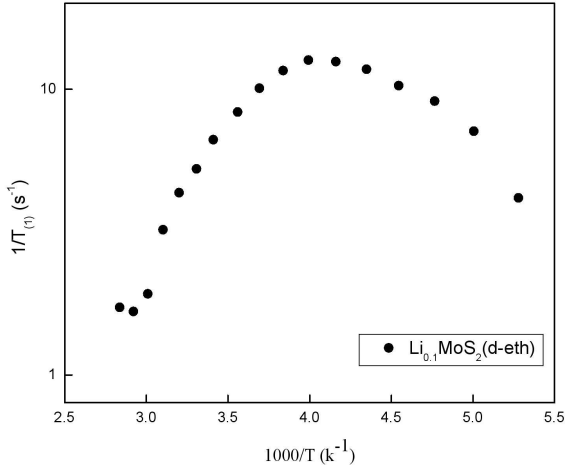
FIG. 4: Temperature dependence of the ^{7}Li spin-lattice relaxation rates (T_1^{-1}) in the $Li_{0.1}MoS_2$[d-eth] nanocomposite, measured at the Larmor frequency 155.4 MHz.

^{7}Li nuclei and the fluctuating electric field gradient produced by the surrounding electrical charge distribution at the nuclear site, and (ii) the dipolar relaxation $(T_1^{-1})_{dip}$ produced by random fluctuations of the lithium homo and heteronuclear dipole-dipole interactions,

$$T_1^{-1} = \left(T_1^{-1}\right)_{dip} + \left(T_1^{-1}\right)_Q \tag{1}$$

The classical theory of the temperature dependence of the spin-lattice relaxation time is given by Bloembergen-Purcell-Pound (BPP) and assumes non-correlated isotropic random motions, yielding to a pair-pair spin correlation function of exponential form, $G(t) = exp(-t/\tau)$, parameterized by the correlation time τ, which defines the time scale for changes of the local magnetic field experienced by the resonant nucleus [26]. In this context, the spectral density function, $J(\omega)$, given by the Fourier transform of the related correlation function, results

$$J(\omega) = \frac{\tau}{1 + (\omega\tau)^2} \tag{2}$$

The experimentally observable spin-lattice relaxation rate can be expressed in terms of the spectral density function evaluated at the NMR Larmor frequencies ω_o of the nuclei [26]:

$$\frac{1}{T_1} = C[J(\omega_o) + 4J(2\omega_o)] \tag{3}$$

The value of the constant C depends on the particular spin interaction responsible for the relaxation. The spectral density function $J(\omega)$ in Eq. (2) is parameterized by the correlation time, τ, of the ionic or molecular motion modulating the nuclear spin interactions.

The dipolar contribution to the spin-lattice relaxation rate can be estimated from the lithium second moment by using the expression

$$\left(\frac{1}{T_1}\right)_{dip} \approx \frac{\gamma^2 M_2}{\omega_o} \tag{4}$$

where $\omega_o = 2\pi$ (155 MHz) $= 9.76\times10^8$ s^{-1} is the ^{7}Li Larmor frequency. Considering the second moment, M_2 (Li) ≈ 4.8 G^2 obtained from the Gaussian line shape of the central line (linewidth 8.5 kHz) of the $Li_{0.1}MoS_2$[d-eth] nanocomposite, it follows that $(T_1^{-1})_{dip} \approx 0.5$ s^{-1}. The quadrupolar contribution to the spin-lattice relaxation rate can be estimated by considering the linewidth of the broad ^{7}Li base line in Fig. 1, which is a reasonable measurement of the theoretical satellites separation. The quadrupole coupling constant $(e^2qQ/\hbar)$ is then estimated to be of the order of 60 kHz [18]. The quadrupolar constant in Eq. (3) is given by

$$C_q = \frac{3\pi^2}{10}\frac{2I+3}{I^2(2I+1)}\left(\frac{e^2qQ}{\hbar}\right)^2 \tag{5}$$

Eq. (5) yields $C_q \approx 10^{10}$ s^{-2}. Since Eqs. (2) and (3) predict that T_1^{-1} should display a symmetric maximum at a temperature at which the condition $\omega_o\tau = 0.62$ is fulfilled, the quadrupolar contribution to the spin-lattice relaxation rate is estimated to be $(T_1^{-1})_Q \approx (1.4)C_q/\omega_o \approx 14$ s^{-1}, yielding $T_1^{-1} = (T_1^{-1})_{dip} + (T_1^{-1})_Q \approx 14.5$ s^{-1}. This result is in good agreement with the experimentally measured relaxation value at the rate maximum, $T_1^{-1} \approx 13$ s^{-1} (Fig. 4). This simple calculation confirms that the quadrupolar interaction is the dominant relaxation mechanism for the ^{7}Li spin-lattice relaxation in the nanocomposite $Li_{0.1}MoS_2$[d-eth]. The same conclusion is valid for the others dialkylamine nanocomposites studied here, since their ^{7}Li spectra exhibit similar base linewidth (i.e., they have comparable quadrupole coupling constants).

No consideration was given here to the dimensionality effects in the lithium nuclear relaxation of these nanocomposites. In the case of dynamical processes in a reduced dimensionality, which is relevant in the case of intercalated species in layered structures, the spectral density function is given by [27-29]:

$$J(\omega_o) = \tau\ln(1 + \frac{1}{\omega_o^2\tau^2}) \tag{6}$$

In contrast to the three-dimensional dynamics, where in the limit $\omega_o\tau << 1$ the relaxation rate is independent of ω_o, a logarithmic frequency dependence for two-dimensional motions is predicted from Eq. (6). In this case, Eq. (3) predicts a maximum in T_1^{-1} when $\omega_o\tau \approx 0.3$, which, in essence, does not alter the estimation of the dipolar and the quadrupolar contribution to the spin-lattice relaxation performed above.

We turn now, to the correlation time of the lithium in the nanocomposites. A remarkable feature of the relaxation data in Fig. 4 is that the ^{7}Li NMR relaxation reaches a maximum

rate at $T_{max} \approx 245$ K. It should be noticed that, in lithium ionic conductors and polymer electrolytes, the ^{7}Li relaxation rate maximum is mostly observed above 300 K when measurements are performed at 155 MHz [5]. It is clear that the position of the T_1^{-1} maximum in Fig. 4 indicates that the lithium mobility in the $Li_{0.1}MoS_2$[d-eth] nanocomposite is high when compared to that of other ionic conductors. The simplest model for the motional correlation time τ is to assume an Arrhenius relationship,

$$\tau = \tau_0 \, e^{\frac{E_A}{k_B T}} \qquad (7)$$

were k_B is the Boltzmann constant, E_A is the activation energy for the process and τ_o^{-1} is the attempt frequency of the order of an optical phonon frequency (10^{12}-10^{13} s^{-1}). The activation energy, calculated from the linear slope of the ^{7}Li T_1^{-1} curve in Fig. 4, yields $E_A = 0.18$ eV and, from the condition for the maximum relaxation rate, a value of $\tau_o \approx 2 \times 10^{-13}$ s is obtained for the pre-factor in Eq (7). Therefore, the correlation time of the lithium motion in the $Li_{0.1}MoS_2$[d-eth] nanocomposite at 300 K is $\tau \approx 2 \times 10^{-10}$ s. Very short correlation times are typical of fast exchange processes. Thus, it seems reasonable to conclude that the lithium atoms are undergoing a fast exchange between the lithium cluster sites. This was the basic argument used in our previous work to identify the motional mechanism in the [d-eth] nanocomposite [18]. For the others two nanocomposites studied here, the measured ^{7}Li relaxation data (not shown in Fig. 4) indicate that the relaxation maxima are shifted towards higher temperature indicating lower lithium mobility than those in the [d-eth] nanocomposite. This behavior is consistent with the ^{7}Li motional narrowing data, where the transition temperature of the first nanocomposite occurs at higher temperature than those of the other ones (Fig. 3). The lithium exchange rate in the [d-eth] nanocomposite was estimated to be $\kappa = (3\tau)^{-1} \approx 320$ MHz at 300 K [18]. A rough estimate suggest exchange rates of the order of 800 – 1000 kHz and 100 kHz at the same temperature for the [d-but] and the [d-pn] nanocomposite, respectively. Fast exchange process was also detected by ^{7}Li T_1 measurements in a solid tetrameric form of *tert*-butyllithium, where the lithium atoms exchange between the four apical sites of a tetrahedron with an exchange rate of 135 MHz at 300 K [24]. Localized exchange of Li between contiguous sites of the perovskite structure was also detected by ^{7}Li relaxation in the fast ionic conductor $Li_{0.18}La_{0.61}TiO_3$ between 220 and 273 K [4].

It is apparent from our NMR data that there is a correlation of the lithium mobility in the three dialkylamine nanocomposites with the corresponding amine size (i.e., the carbon number in the amine species, n in the amine group [C_nH_{2n+2}NH]). Both the ^{7}Li NMR linewidth and relaxation data suggest that the lithium exchange rate became smaller in the nanocomposites with larger amines. The gradual decrease in exchange rate seems to be related to the packing effects resulting from the intercalation of the large amines molecules. Further work is in progress to obtain a more accurate characterization of this behavior.

The ^{7}Li spin-lattice relaxation analysis presented above illustrates the importance of the nuclear spin relaxation methods in determining motional parameters and probing the mechanisms responsible for the ion dynamics. The first step in the interpretation of NMR relaxation data was to determinate the interactions responsible for the relaxation processes. The results show that the fluctuations of the quadrupolar interaction due to the Li$^+$ motions is the dominant mechanism responsible for the ^{7}Li spin-lattice relaxation in the nanocomposites studied here.

IV. CONCLUSIONS

In this contribution we emphasize that NMR is a very powerful tool for studying molecular architecture and lithium dynamics. The systems studied here were nanocomposites formed by the co-intercalation of lithium and dialkylamines in molybdenum disulphide. The NMR line shape and relaxation times of ^{7}Li resonance indicated the formation of self-assembled Li$_3$ clusters stabilized by amine ligands within the interlaminar space of this intercalation compound. The model has the advantage of being consistent with the geometrical restriction imposed by the intercalation space between host layers. The ^{7}Li NMR measurements provide strong evidence of the fast lithium exchange within the aggregate and suggest that the lithium mobility is affected by the geometrical restriction resulting from the intercalation of the amine molecules.

[1] H. Eckert, Progress NMR Spectroscopy **24**, 159 (1992).

[2] E. R. Andrew, E. Szczesniak, Progress NMR Spectroscopy **28**, 11 (1995).

[3] S. Sen, J. F. Stebbins, Physical Review B **55** (6) 3512 (1997)

[4] M. A. París, J. Sanz, C. León, J. Santamaría, J. Ibarra, and A. Várez, Chem. Mater. **12**, 1694 (2000).

[5] P. Mustarelli, C. Capiglia, E. Quartarone, C. Tomasi, P. Ferloni, and L. Linati, Phys. Rev. B **60**, 7228 (1999).

[6] S. H. Chung, K. R. Jeffrey, and J. R. Stevens, J. Chem. Phys. **94** (3) 1803 (1991).

[7] B. Scrosati, Nature **373**, 557 (16 February 1995).

[8] J. M. Tarascon, M. Armand, Nature **414**, 359 (15 November 2001).

[9] C. Julien, G. A. Nazri, *Solid State Batteries: Materials, Design and Optimization* (Kluwer Academic, Boston, 1994).

[10] T. Pietrass, F. Taulelle, P. Lavela, J. Olivier-Fourcade, J.C. Jumas, and S. Steuernagel, J. Phys. Chem. B **101**, 6715 (1997).

[11] R. Bertermann, W. Müller-Warmuth, C. Jansen, F. Hiltmann, and B. Krebs, Solid State Ionics **117**, 245 (1999).

[12] R. Winter, P. Heitjans, J. Phys. Chem. B **105**, 6108 (2001).

[13] Y. Paik, C. P. Grey, C. S. Johnson, J-S. Kim, and M. M. Thackeray, Chem. Mater. **14**, 5109 (2002).

[14] P. E. Stallworth, F. S. Johnson, S. G. Greenbaum, S. Passerini, J. Flowers, and W. Smyrl, J. Applied Physics **92**, 3839 (2002)

[15] G. P. Holland, D. A. Buttry, and J. L. Yarger, Chem. Mater. **14**, 3875 (2002).

[16] R. Fu, Z. Ma, J. P. Zheng, G. Au, E. J. Plichta, and Ch. Ye, J. Phys. Chem. B **107**, 9730 (2003).

[17] E. Benavente, M. A. Santa Ana, F. Mendizábal, and G. González, Coordination Chem. Reviews **224**, 87 (2002).

[18] A. C. Bloise, J. P. Donoso, C. J. Magon, J. Schneider, H. Panepucci, E. Benavente, V. Sanchez, M. A. Santa Ana, and G. González, J. Phys. Chem. B **106**, 11698 (2002)

[19] V. Sanchez, E. Benavente, M. A. Santa Ana, and G. Gonzalez, Chemistry of Materials **11**, 2296 (1999).

[20] M. E. Smith, E. H. R. Van Eck, Progress NMR Spectroscopy **34**, 159 (1999).

[21] E. Benavente, M. A. Santa Ana, G. Gonzalez, F. Becker-Guedes, N. C. Mello, H. Panepucci, T. J. Bonagamba, and J. P. Donoso, Electrochimica Acta **48**, 1997 (2003).

[22] S. E. Hayes, R. A. Giodotti, W. R. Even, P. J. Hughes, and H. Eckert, J. Phys. Chem. A **107**, 3866 (2003).

[23] R. Setton, J. Conard, Mol. Cryst. Liq. Cryst. **244**, 307 (1994).

[24] G. H. Penner, Y. C. Phillis Chang, Chem. Comm. 1803 (2000).

[25] C. C. Tambelli, J. P. Donoso, C. J. Magon, L. A. Bueno, Y. Messaddeq, S. L. J. Ribeiro, L. F. C. Oliveira, and I. Kosacki, J. Chem. Phys. **120**, 9638 (2004).

[26] A. Abragam, *Principles of Nuclear Magnetism* (Oxford University Press, London, 1961).

[27] P. M. Richard, in: *Physics of Superionics Conductors*, Topics in Current Physuics, Ed. M. B. Solomon (Springer, Berlin, 1979). P. 111.

[28] C. Berthier, Y. Chabre, P. Segransan, Physica B **99**, 107 (1980).

[29] D. Brinkmann, Magnetic Resonance Review **14**, 101, (1989); Progress NMR Spectroscopy **24**, 527 (1992).